

Robust Cross-point Metal Oxide Resistive Memory Design with Hard Error and Soft Error Resilience

Abstract—The transition metal oxide (TMO) resistive random access memory (ReRAM) has been identified as one of the most promising candidates for the next generation non-volatile memory (NVM) technology. Numerous TMO ReRAMs with different materials have been developed and show attractive characteristics, such as fast read/write speed, long retention time, low power consumption, high integrated density, and good scalability. In addition, the unique non-linearity of some ReRAMs provides the possibility to build a cross-point structure based ReRAM array, which further improve the area efficiency.

However, the existence of sneak current and voltage drop along the interconnection metal wire bring in extra design challenges. In addition, similar to other NVM technologies, such as Phase Change Memory (PCM) and Spin-Transfer Torque RAM (STT-RAM), the ReRAMs also suffer from soft and hard cell errors. In this paper, we summarized mechanisms of both soft and hard errors of ReRAM cell and a unified model is proposed to characterize the failure behaviors. Based on the study, circuit-level and architecture-level resilience design are proposed. Our simulation results show that, XXXXXXXXXXXX.

I. INTRODUCTION

The resistive switching phenomenon of metal oxide materials has been studied for a half-century. The negative resistance has been already observed in some metal-oxide-metal(MIM) structures at early 1960's. Based on the hysteretic resistance switching behaviors, researchers firstly proposed to use the MIM structure for memory applications in 1967 [1], [2]. However, it was not until the early 21st century that the practical ReRAM application has been fabricated [3], [4]. The oxide materials evolve from complex perovskite oxides to more easily fabricated binary TMO at early 2000's. The advantages of TMOs, such as good compatibility to CMOS processes and thermal/chemical resilience, make TMOs the most competitive materials for MIM structure ReRAM cell. Many TMOs was tested in Baek's work [4] and the fully CMOS technology compatible, NiO based ReRAM was demonstrated with operation voltage below 3V and switching current below 2mA. After that, a bunch of TMO based ReRAM with various materials, such as CuOx, WOx, HfOx, TiOx, and TaOx, have been demonstrated [5], [6], [7], [8], [9], [10]. These TMO based ReRAMs have shown excellent features, including low power, fast access speed, small cell size, good scalability, as well as back-end-of-the-line (BEOL) CMOS process compatibility. For example, Panasonic published a paper at the International Solid-State Circuit Conference (ISSCC) this year that presented a multi-layer ReRAM macro with 443MB/s throughput at 8.2ns pulse width [10]. XXXXXXXXXXXXXXXXXXXXXXXX considered as a

Traditional memory technologies, such as SRAM, DRAM, and FLASH, suffers from both soft errors and hard errors. The soft error is a random, recoverable upsetting of the information store in memory cell, while the hard error is a permanent corruption of the memory cell results from physical defect. Although the emerging non-volatile memory technologies are not charge-based storage, they also suffer from the soft error and hard error results from the physical characteristics of the cell. The presence of hard error normally results from the limited endurance compared to DRAM and SRAM technologies. However, the cause of soft error is distinctive for each NVM. For example, the soft error of Phase-Change Memory

(PCM) comes from the resistance shift behaviors of the amorphous phase of chalcogenide materials, as well as the thermal disturbance from adjacent cells. For Spin-Transfer Torque RAM (STT-RAM), the stochastic properties implies that both of the write and read operation can bring in soft error. Similar to other NVM technologies, the ReRAM also suffers from the soft errors and hard errors originated from different physical mechanisms. Specifically, the soft errors of ReRAM cell result from the retention failures of the cell. And the hard error always comes from the limited endurance of the cell. In the presence of both the soft errors and hard errors, the reliability of ReRAM array, especially for the most area/cost efficient cross-point structure ReRAM array, becomes a serious design challenge. In this work, we systematically summarized the mechanism of both soft and hard errors of ReRAM cell and proposed a unified model to characterize the failure behaviors of different types of hard errors. By using the model, the impact of soft and hard errors on the cross-point ReRAM array is detailed studied.

The remainder of the paper is organized as follows. In Section II, the background of the metal oxide ReRAM cell and cross-point architecture is introduced. xxxxxx. The experimental results and discussion are provided in Section V. We conclude our work with Section VI.

II. PRELIMINARY

In this section, the background of TMO ReRAMs are presented. Specifically, the resistance switching mechanisms of unipolar and bipolar ReRAM cell are introduced in detail. Then the cross-point architecture of ReRAM array is detailed.

A. Metal Oxide Resistive Memory

The resistance switching behavior is observed in many materials, such as perovskite oxides, transition metal oxides, solid-state electrolytes, and organic materials. Among all of these materials, the TMO MIM structures attracted lots of research interests not only because its good electrical characteristics, such as fast access speed, high ON-OFF resistance ratio and low power consumption, but also because of is good scalability, 3-D stackability, as well as BEOL CMOS process capability.

A schematic view of the MIM structure of TMO based ReRAM cell is shown in Fig. 1(a). The ReRAM cell has a very simple structure: a TMO based storage layer sandwiched by two metal layers of electrodes, named top electrode (TE) and bottom electrode (BE). As implied by its name, the ReRAM cell uses the resistance to represent the information stored in the cell: low resistive state (LRS or ON-state) and high resistive state (HRS or OFF-state) are used to represent the logic '1' and '0' respectively. As shown in Fig. 1(a), in order to switch a ReRAM cell between the LRS and the HRS, a external voltage with specified polarity, magnitude, and duration is required. According to the switching behaviors, the ReRAM can be classified into two category: the bipolar and the unipolar ReRAM. For the unipolar ReRAM cell, the resistance switching only depends on the magnitude of the external voltage applied across the cell,

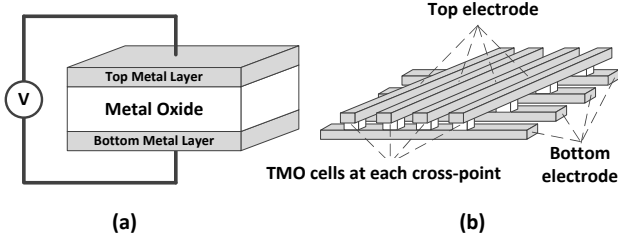


Fig. 1. An overview of (a) TMO MIM structure and (b) a cross-point ReRAM array.

independent of the polarity of the voltage. On the other hand, for the bipolar ReRAM cell, the LRS-to-HRS switching (aka RESET operation) and the HRS-to-LRS switching (aka SET operation) occur at different polarities. In addition to SET and RESET operation, the forming operation is another important process for the ReRAM cell. Briefly, the forming operation is the first SET operation, which switch a fresh device into LRS by a soft dielectric breakdown. After the forming process, the device can be switched between LRS and HRS repeatedly. The demand of forming operations brings extra challenges and overheads to the ReRAM design since it always requires larger voltage/current than SET/RESET operation. Fortunately, researchers figured out that the forming voltage can be reduced linearly with the decrease of the thickness of the TMO thin film[cite]. Besides, the forming voltage can be also reduced by improving the deposition process[cite]. Recently, several forming-free ReRAMs have been proposed[[]]. The switching and forming mechanisms will be discussed in Section III-B. A variety of TMOs have already show the potential as the insulator layer of the MIM structure non-volatile ReRAM cell with different electrical characteristics such as operation voltage, switching speed, endurance, and retention time. Wong [11] provided a comprehensive review of metal-oxide ReRAM with detailed discussion of HfO_x , AlO_x , NiO , TiO_x , and TxO_x based devices. However, in this paper, we will not focus on the different materials of the ReRAM cell. Conversely, we will study the general reliability issues, such as endurance failures and retention failures, that exist almost in all of the TMO based ReRAM.

B. Memory Structure of ReRAM Array

Almost all of the random access memories are organized as a matrix-like structure: one memory cell along with its access device (normally a MOSFET) are located in each intersection of horizontal wordlines and vertical bitlines. Similarly, the ReRAM array is also has this NOR-type structure. There are two potential structures of a ReRAM array: the MOSFET-accessed structure (1T1R structure) and the cross-point structure. In the MOSFET-accessed structure, each ReRAM cell has a dedicated MOSFET as its access device. The advantage of this structure is that it is very easy to control each cell in the array independently without crosstalk results from the sneak current in cross-point structure. However, in the MOSFET-accessed structure, the size of the MOSFET should be designed large enough to satisfy the current requirement of the SET/RESET operation. Therefore, the total area of the ReRAM array often determined by the access devices instead of the ReRAM cells, which seriously harmed the area advantage of the ReRAM devices. On the other hand, the cross-point structure is a more area efficient structure compared to MOSFET-accessed structure. As shown in Fig. 1(b), in the cross-point structure, each ReRAM cell is sandwiched by TE and BE at each cross-point of the array without access device. In this structure,

each cell only occupy an area of $4F^2$ (F is the feature size of the fabrication technology), which is the theoretical smallest cell area for a single layer single level memory array. For example, Hynix and HP Labs has already demonstrated a 2Mb $4F^2$ cross-point ReRAM chip based on 54nm technology [8]. In addition, the good 3-D stackability can further reduce the effective cell area. An 64MB $0.5F^2$ cross-point CMOx ReRAM chip was demonstrated by Unity Semiconductor at 2010 [12].

As mentioned, the write operations (SET and RESET) of a ReRAM cell require external voltage across the cell with specified magnitude and duration. To write a cell in the cross-point array, the wordline and bitline where the cell located should be activated at specified write voltage. In addition, all of the unselected wordlines and bitlines are set to a certain voltage or left floating to guarantee that all of the unselected cells are not disturbed. There are several write schemes of the cross-point array. One of the most common scheme for bipolar cross-point array is called HWHB scheme: during the write operation, the selected wordline and bitline are activated at write voltage V_{write} or 0, while all of the unselected wordlines and bitlines are half biased at $V_{write}/2$. In this scheme, the write voltage V_{write} or $-V_{write}$ is fully applied across the selected cell. The other cells located at the same wordline and bitline with the selected cell are half biased at $V_{write}/2$. And there are no voltage drop across all of the other cells. However, even with proper write schemes, the sneak current at the half selected cells are significant. For a 512×512 array, the sneak current is more than 500 times larger than the SET/RESET current, bring in huge area overhead of the voltage drivers and unnecessary energy consumption at the half selected cells. Therefore, in order to implement a practical cross-point array with acceptable overhead, a large nonlinearity of the ReRAM cell is essential. The resistance of a ReRAM cell with nonlinearity increases with the reducing of applied voltage. In this case, the sneak current at half selected cells will be reduced significantly. The read operation is to bias the selected wordline at V_{Read} and ground all of the other wordlines and bitlines. Then the state of the selected cell is read out by sense amplifier connected to the selected bitline.

Although the cross-point structure suffers from aforementioned shortcomings, its area efficiency is an attractive superiority compared to other emerging NVMs. In addition, the BEOL CMOS process capability makes it possible to implement the array on top of (part of) the peripheral circuitry, further improving the area efficiency. Since the chip area is directly related to the cost-per-bit metric, the cost advantage make the cross-point ReRAM a promising candidate for DRAM or FLASH replacement.

III. IMPACT OF CELL ERRORS ON CROSS-POINT ReRAM DESIGN

Reliability is a vital concern in the design of memory system. In the cross-point structure, the reliability issues comes from two different sources: **structural error** and **cell error**. The structural error comes from the special organization of the cross-point array. The impact of voltage drop, sneak current, write/read schemes, as well as data pattern on the array reliability are well studied in literatures [13], [14]. It has been shown that the structural errors can be mitigated or eliminated with exhaustive worst-case design. On the other hand, because of the intrinsic characteristics of ReRAM cells, the impact of cell errors is not avoidable. To implement a reliable ReRAM array, additional detection and recovery mechanisms and circuitry are required. In this section, we first discussed the resistance switching behaviors of ReRAM cell. Based on the discussion, mechanisms and modeling of soft error and hard error of ReRAM cell is presented. Then, the impact of the cell errors at the array design is evaluated.

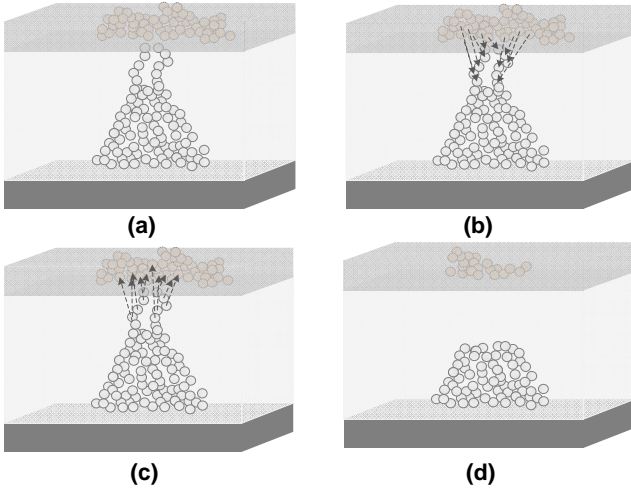


Fig. 2. (a) LRS of the ReRAM cell after the formation or SET operation. (b) RESET operation. (c) HRS of the ReRAM cell after RESET operation. (d) SET operation.

A. ReRAM resistance switching mechanisms

There are several studies have been conducted to reveal the physical mechanisms of the resistance switching behaviors. Recently, the filamentary model is widely accepted to explain the resistance switching phenomenon in the TMOs ReRAM: switchings between LRS and HRS are caused by the formation and rupture of the nanoscale conductive filaments (CFs) at the anode interface of the cell. For forming operation can be considered as a 'preset' operation of the ReRAM cell. The schematic view of the switching mechanisms of ReRAM cell is illustrated in Fig. 2.

During the forming step, a high voltage is applied across the cell. The dielectric soft breakdown in the materials generates a great amount of the defects in the TMOs, which form one or several CFs through the cell. At the same time, the anode becomes a reservoir of the oxygen ions. After the forming operation, the cell exhibit LRS, which is shown in Fig. 2(a). The RESET operation is shown in Fig. 2(b). In this step, the oxygen ions are forced back to the TMO layer by the electric field and recombine with the oxygen vacancies (Vo). In this case, the CFs are "cut off" and the cell becomes HRS, which is shown in Fig. 2(d). In contrast, the SET operation can be considered as a converse process of the RESET operation. As shown in Fig. 2(c), the SET operation realizes the regeneration of the CFs by separating the oxygen ions and the Vo again. In this case, the cell switches back to the LRS.

B. Mechanisms and Modeling of Soft Error and Hard Error of ReRAM

Soft error of the ReRAM cell come from the retention error. The retention failure is a recoverable upset of the resistance of the cell. The retention failure can either be a suddenly resistance drop of the HRS cell (HRS failure) or a suddenly resistance increasing of the LRS cell (LRS failure). The retention failure behaviors result from the random generation of the Vo (HRS failure), and the recombination of Vo with oxygen ions (LRS failure). Both of them imply that the retention failure is a random phenomenon rather than a cumulative phenomenon. Since either of the HRS failure or the LRS failure can be the dominate soft error of the ReRAM with different materials and process technology [15], [16], in this paper, we focus on the soft error that dominated by the LRS failure.

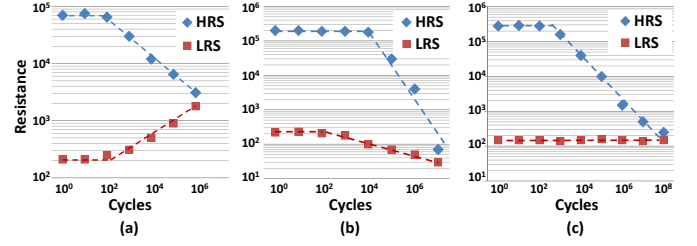


Fig. 3. Hard errors in TMO ReRAM cell: (a) Type I, (b) Type II, and (c) Type III endurance failure.

In order to quantify the retention failure behavior, the cumulative failure probability is employed. A simplified model of the cumulative failure probability is proposed by Gao [16], which can be expressed as

$$F(t) = 1 - (1 - p)^{(\alpha t)}, \quad (1)$$

where α is a constant value, t is the retention time, and p is the generation probability of the Vo and has the term of

$$p_H = \exp((qVl/2d - \varepsilon_V)/kT), \quad (2)$$

where q is the electric quantity of the oxygen ions, V is the applied voltage on the TMO layer, l is the lattice constant, d is the length of the filament's ruptured region, and the ε_V is the oxygen vacancy's formation energy.

Different from soft error, the hard error results from the limited endurance of the ReRAM cell compared to traditional DRAM/SRAM technologies. The endurance failure is caused by a gradually resistance change over the write cycles. According to different behaviors and physical mechanisms, the endurance failures are classified into three categories [17]:

- 1) Type I Failure: This failure is caused by the generation of extra oxide layer at the anode during the SET operations. This layer prevents the moving of the oxygen ions and results in the increased R_{LRS} and the decreased R_{HRS} .
- 2) Type II Failure: The programming voltage generated extra Vo, which directly increases the diameter of the CFs. In this failure, both of the R_{LRS} and the R_{HRS} decreases gradually.
- 3) Type III Failure: This failure results from the undesired consumption of the oxygen ions at stored in the anode. In this case, the combination probability of Vo and oxygen ions will reduce. Thus the R_{HRS} decreases while the R_{LRS} keeps constant.

For simplicity, we proposed a unified model to summarize these three types of endurance failure as

$$R = R_0(1 + \alpha_0(t - t_0)^\xi(\text{sgn}(t - t_0) + 1)/2), \quad (3)$$

where R_0 is the initial resistance of LRS or HRS, t_0 is the start point that the endurance degradation is observed, and α_0 and ξ represent the direction and speed of the resistance change. The model with different parameters fits good with the published data and is shown in Fig. 3 as dash lines.

C. Impact of Soft and Hard Error on Cross-point Array

The soft error is a recoverable error and represents as a HRS-to-LRS or LRS-to-HRS transition. Therefore, we conclude that soft errors can only affect the information stored in the cells where the endurance failures arise, and will not affect the other cells in the cross-point array. To overcome the soft error, the Error Correction Code (ECC) is necessary. The area, energy, and latency overheads will be evaluate in Section V.

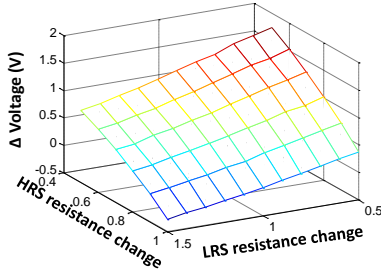


Fig. 4. Impact of endurance failures on read margin.

Compared to the soft errors, the hard errors are more serious, especially for the cross-point structure. In general, the impact of hard errors exists in two aspects: (1) the degradation of the read margin results from the shrink of the resistance ratio between the HRS and the LRS. This problem appears in all of three types hard errors; (2) the design overhead that incurred by the hard errors, including the area overhead, energy consumption overhead, as well as more severe array size limitation. However, since the LRS is the decisive for the worst-case design, only the Type II hard error will affect the design.

Fig. 4 shows the read margin degradation results from the resistance change of the HRS and LRS. According to the aforementioned Type I-III hard errors, the endurance failures of HRS always represent the resistance reduction. However, the resistance of LRS may either increase (for Type I error) or decrease (for Type II error). Therefore, in this figure, we assume the resistance of HRS can reduce to half of the original value, while that of LRS can either increase or decrease by 50% of the original value. From the figure, we can see that the reduction of the resistance ratio between HRS and LRS, which results from the resistance increasing of LRS and decreasing of HRS, has significant impact on the read margin. For example, when the resistance of LRS reduces by 50%, the read margin will reduce by 35%. And when the resistance of HRS increase by 50%, the read margin shrinks to only 1.2% of the original read margin. This observation indicates that the HRS endurance failure brings more serious degradation to the read noise margin.

As mentioned, to overcome the hard errors, the design limitations of the cross-point array is further deteriorated. To ensure the reliability of the array, the cross-point array is always designed for the worst case - making sure that the array can work reliably, regardless the data pattern in the array. Many researches have been conducted to study the worst case design [13], [14] and it has been figure out that the lowest resistance is the key parameter for the worst case design of cross-point array. Since the LRS resistance reduction is only observed in Type II error, therefore, we conclude the Type II hard error is the key player for the worst case design. Firstly, the limitation of the array size results from the voltage drop along the wordlines and bitlines. Our simulation shows that the decrease of the resistance of LRS will aggravate the voltage drop and therefor reduce the allowable array size. As shown in Fig. 5, the maximum array size reduces from 512 by 512 to 355 by 355 with the LRS resistance drop to half of its original value. Besides, the energy consumption and the driver current are also impact by the LRS resistance reduction. Fig. 6 shows the energy and driver current overhead of the LRS resistance reduction. As shown, the worst case energy consumption of the array increases by 55%. On the other hand, the driver current in increases up to 72%. Since the area of the wordline voltage driver and bitline multiplexors is linearly related to the driver current requirement, the area of peripheral circuits are also harmed.

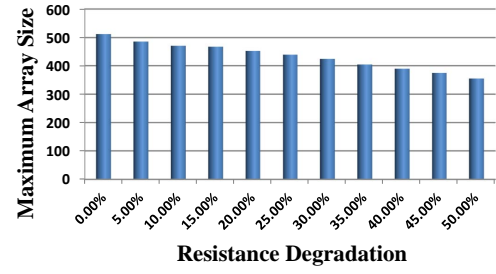


Fig. 5. Impact of Type II error on maximum array size.

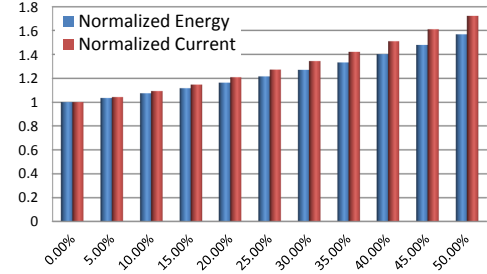


Fig. 6. Impact of Type II error on energy consumption and current requirement.

IV. SOFT ERROR AND HARD ERROR RESILIENCE DESIGN OF ReRAM

As mentioned, in the absence of soft and hard error, the cross-point array

Proposed different level resilience design
circuit-level 2-level ECC + early error detection circuit
architecture-level evict array always write to HRS

V. EXPERIMENTAL RESULTS

The uniformity of the ReRAM cell is a

VI. CONCLUSION

REFERENCES

- [1] J. G. Simmons and R. R. Verderber. New conduction and reversible memory phenomena in thin insulating films. *Proceedings of the royal society A*, 301:77 – 102, 1967.
- [2] C. J. Varker and E. M. Juleff. Electron beam recording in SiO₂ with direct read-out using the electron beam induced current at a p-n junction. *Proceedings of the IEEE*, 55(5):728 – 729, 1967.
- [3] W.W. Zhuang et al. Novel colossal magnetoresistive thin film nonvolatile resistance random access memory (rram). In *Electron Devices Meeting, 2002. IEDM '02. International*, pages 193 –196, 2002.
- [4] I.G. Baek et al. Highly scalable nonvolatile resistive memory using simple binary oxide driven by asymmetric unipolar voltage pulses. In *Electron Devices Meeting, 2004. IEDM Technical Digest. IEEE International*, pages 587 – 590, 2004.
- [5] Tzu-Ning Fang et al. Erase mechanism for copper oxide resistive switching memory cells with nickel electrode. In *Electron Devices Meeting, 2006. IEDM '06. International*, pages 1 –4, 2006.
- [6] ChiaHua Ho et al. 9nm half-pitch functional resistive memory cell with 1lua programming current using thermally oxidized sub-stoichiometric wox film. In *Electron Devices Meeting (IEDM), 2010 IEEE International*, pages 19.1.1 –19.1.4, 2010.
- [7] Y.S. Chen et al. Highly scalable hafnium oxide memory with improvements of resistive distribution and read disturb immunity. In *Electron Devices Meeting (IEDM), 2009 IEEE International*, pages 1 –4, 2009.
- [8] Hyung Dong Lee et al. Integration of 4f2 selector-less crossbar array 2Mb ReRAM based on transition metal oxides for high density memory applications. In *VLSI Technology (VLSIT), 2012 Symposium on*, pages 151 –152, june 2012.

- [9] Shyh-Shyuan Sheu et al. A 4mb embedded slc resistive-ram macro with 7.2ns read-write random-access time and 160ns mlc-access capability. In *Solid-State Circuits Conference Digest of Technical Papers (ISSCC), 2011 IEEE International*, pages 200 –202, feb. 2011.
- [10] A. Kawahara et al. An 8mb multi-layered cross-point rram macro with 443mb/s write throughput. In *Solid-State Circuits Conference Digest of Technical Papers (ISSCC), 2012 IEEE International*, pages 432 –434, feb. 2012.
- [11] H.-S.P. Wong, Heng-Yuan Lee, Shimeng Yu, Yu-Sheng Chen, Yi Wu, Pang-Shiu Chen, Byoungil Lee, F.T. Chen, and Ming-Jinn Tsai. Metal-oxide rram. *Proceedings of the IEEE*, 100(6):1951 –1970, june 2012.
- [12] C.J. Chevallier et al. A 0.13 um 64mb multi-layered conductive metal-oxide memory. In *Solid-State Circuits Conference Digest of Technical Papers (ISSCC), 2010 IEEE International*, pages 260 –261, feb. 2010.
- [13] J. Liang and H.-S.P. Wong. Cross-point memory array without cell selectors - device characteristics and data storage pattern dependencies. *Electron Devices, IEEE Transactions on*, 57(10):2531 –2538, oct. 2010.
- [14] Dimin Niu et al. Design trade-offs for high density cross-point resistive memory. In *Proceedings of the 2012 ACM/IEEE international symposium on Low power electronics and design, ISLPED '12*, pages 209–214, New York, NY, USA, 2012. ACM.
- [15] Shimeng Yu, Yang Yin Chen, Ximeng Guan, H.-S. Philip Wong, and Jorge A. Kittl. A monte carlo study of the low resistance state retention of hfox based resistive switching memory. *Applied Physics Letters*, 100(4):043507, 2012.
- [16] Bin Gao, Haowei Zhang, Bing Chen, Lifeng Liu, Xiaoyan Liu, Ruqi Han, Jinfeng Kang, Zheng Fang, Hongyu Yu, Bin Yu, and Dim-Lee Kwong. Modeling of retention failure behavior in bipolar oxide-based resistive switching memory. *Electron Device Letters, IEEE*, 32(3):276 –278, march 2011.
- [17] B. Chen, Y. Lu, B. Gao, Y.H. Fu, F.F. Zhang, P. Huang, Y.S. Chen, L.F. Liu, X.Y. Liu, J.F. Kang, Y.Y. Wang, Z. Fang, H.Y. Yu, X. Li, X.P. Wang, N. Singh, G.Q. Lo, and D.L. Kwong. Physical mechanisms of endurance degradation in tmo-rram. In *Electron Devices Meeting (IEDM), 2011 IEEE International*, pages 12.3.1 –12.3.4, dec. 2011.